Error Structure Arising from the Synchronization of Hybrid Chaotic Systems with Mixed Time Delays

Morris H. Morgan[1], Carolyn B. Morgan[2], Kristin D. Morgan[3]
[1]Hampton University, Queen and Tyler Streets, Hampton, VA 23185
[2]Hampton University, Queen and Tyler Streets, Hampton, VA 23185
[3]University of Kentucky, 900 S. Limestone Street, Lexington, KY 40536

Abstract

Past research has been successful in identifying a robust statistical error-based controller for synchronizing chaotic systems with and without inherent time delays. However, for an arbitrary time delay, neither local nor global stability is a certainty. Care must be taken to identify such stability pockets prior to implementing the statistical error-based controller design (SEBCD) strategy. These hybrid systems arise in many physical and biological settings and impose additional constraints on controller design. Our new approach involves generating initial (zero-state) error distributions based on differences between the response and drive signals. The differences are used to estimate stability limits and controller gains only within these stable pockets. In the present investigation, autoregressive integrated moving average (ARIMA) models of these synchronization errors are used to develop graphical stability maps that highlight the connections among controller gains and the spectral nature of the resulting ARIMA coefficients.

Key Words: Controller, ARIMA, synchronization, time delay, robust, chaotic

1. Overview

In previous investigations the robustness of a statistical controller originally devised for synchronizing chaotic oscillators has been studied. Later research has extended this work to hybrid systems that involved coupling functional ordinary differential equations to such chaotic system. Such time delay hybrid systems paired a functional system with a chaotic oscillator. These systems arise in many practical settings where there is a dependence on past state information. Two classical examples of delay systems are the Mackey-Glass (1977) and Marcus and Westervelt (1989) equations. Hence, for an arbitrary time delay local or global stability is not a certainty. Care must be taken to identify those stable zones prior to implementing the statistical error-based controller design (SEBCD) procedure. Studies of such complex systems highlighted the efficacy of SEBCD for designing a robust controller using moment estimates. For the Olgac and Sipahi system examined in Morgan & Morgan (2014) those stability pockets were found to lie in the intervals $0<\tau<0.1624$ and $0.1859<\tau<0.2222$. Any cases with delays outside these intervals produce unstable drive dynamics. Nevertheless, synchronization can be achieved despite the fact that the response system tracks the unstable drive to oblivion. Since the same response model is employed here as in Morgan & Morgan (2013 & 2014), the prior statistical error-based controller design applies in the present setting. However, the present paper addresses the role of the resulting gain-error characteristic equation and its impact on error dynamics associated with such coupling designs.

1.1 Approach

The initial step in the analysis involves constructing interval approximations for each nonlinear term in our chaotic model from descriptive statistics of the unsynchronized response system. Thus, armed with these interval estimates, local stability was assessed and used to determine the global stability requirement for a given drive-response combination. Under this paradigm, the stability of the drive system is not necessary for establishing overall system synchronization, only the response is needed. The drive only dictates the path the response system will take. Figure 1a shows the uncoupled dynamic response of a hybrid system (Olgac and Sipahi) prior to synchronization while Figure 1b highlights the influence of the drive on the synchronized response. Note a high level of compression occurs with synchronization and the conversion speed is accelerated. The gain-error characteristic equation examined in this study characterizes the level of fidelity between the drive and response system and is the main focus of the present inquiry.

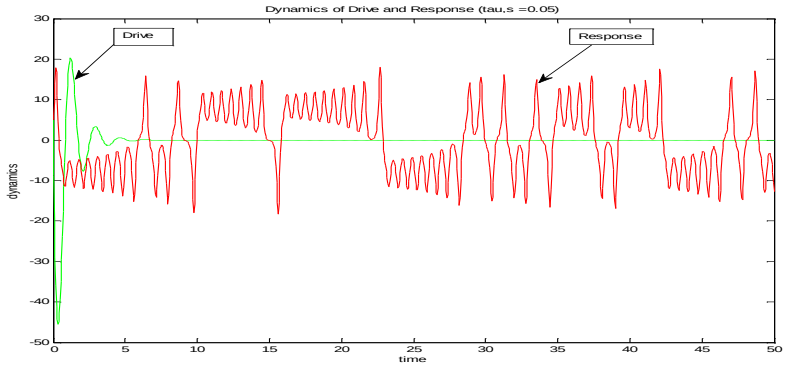

Figure 1a) Dynamic Responses: Uncoupled

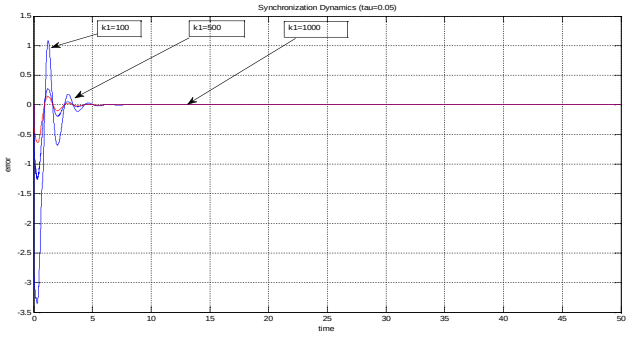

Figure 1 b) Dynamic Responses: Coupled

The basic design philosophy has been outlined in detail in prior papers, Morgan & Morgan (2012, 2013 & 2014). Those approaches removed local nonlinearities via

construction of fuzzy intervals for each nonlinear term appearing in the response system equations. A system of ordinary differential equations were then converted as shown below for the response system into a set of linear interval equations for estimating controller settings from a gain-error characteristic polynomial. Unlike our prior effort in Morgan and Morgan (2012) that followed a design procedure suggested by Bhiwani & Patre (2011) for a classical proportional-integral-derivative (PID) controller, the current approach eliminates a cumbersome optimization step encountered with the former. The constraints imposed in the present design are that all error-based moment gains must be positive and all generated errors are bounded by the initial state errors between the number of controller parameters matches the number of state equations was considered.

EQUATIONS

Original Model	***Extended/Fuzzy Model***
$\frac{dx}{dt} = 10\,(y - x)$	$\frac{dx}{dt} = \left[\,10 - \sum k_{xi}\,\varepsilon_{xi}^{i-1}\right]y \; - 10x$
$\frac{dy}{dt} = -xz + 28\,x - y$	$\frac{dy}{dt} = \left[\,28 - \sum k_{yi}\,\varepsilon_{yi}^{i-1} - z_s\right]x \; - y$
$\frac{dz}{dt} = xy - 2.67\,z$	$\frac{dz}{dt} = \left[\,y_s - \sum k_{zi}\,\varepsilon_{zi}^{i-1}\right]x \; - 2.67\,z$

The gain-error characteristic equation for the Lorenz system takes the following form

$$p(\varepsilon) = (k_1 - C_{max}) + k_2\,\varepsilon + k_3\,\varepsilon^2$$

The C_{max} term appearing in the above equation is the maximum value found from bracketed terms of the interval description of the original Lorenz system. Two distinct solutions are possible based upon the sign of the discriminant associated with the gain-error characteristic polynomial. Interestingly, the sign of the discriminant also dictates the type of image produced. A negative value of this quantity generates overlapped images while a positive one produces displaced images. It was also observed that the k_1 gain controlled the error level between synchronized states, as reported in Morgan and Morgan (2012), and that the regression model developed in that study was applicable for all drive systems linked to this particular Lorenz controller. That analysis revealed the presence of two distinct zones (unstable and stable regions) whose size was bounded by the length of the maximum fuzzy interval while the minimum fuzzy interval enclosed the un-entangled (critical) point.

2. Discussion of Results

Beyond just impacting image patterns, the discriminant (D) was also found to alter the error structure. For discriminant values greater than zero, a diverse collection of non-predictable error patterns arose that were not readily linked in any discernible manner to the controller parameters as highlighted in Figure 2a. However under conditions where the discriminant is less than zero, an emerging pattern evolves. The error structure became sinusoidal and locks into a critical frequency (see Figure 2b). As depicted in Figure 3, increasing the proportional controller gain, k_1, reduced the error signal amplitude but did not alter the critical locking frequency.

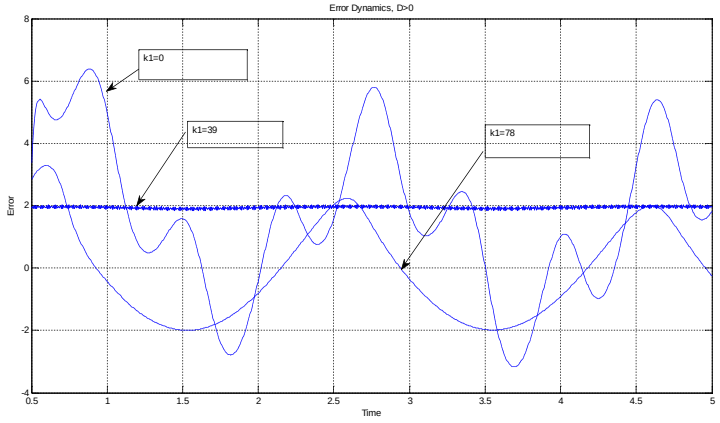

Figure 2a: Dual Image Error Patterns

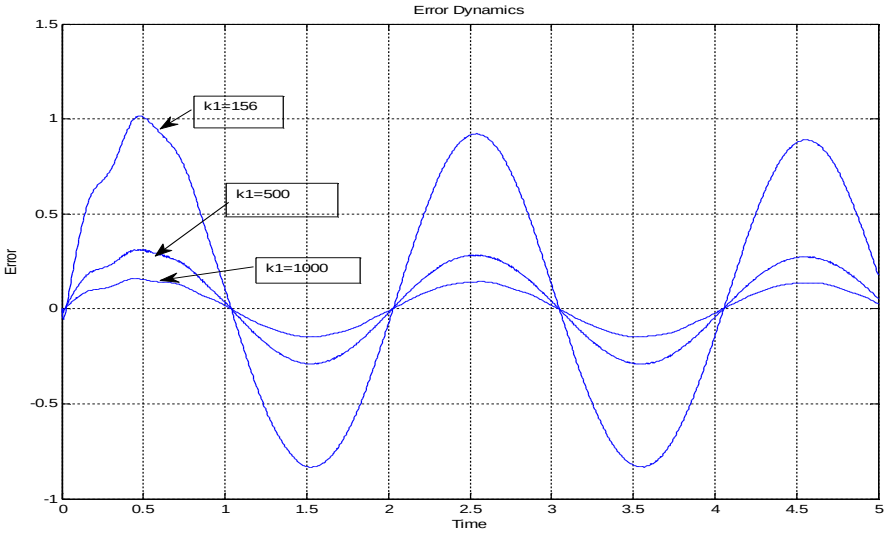

Figure 2b: Single Image Error Pattern

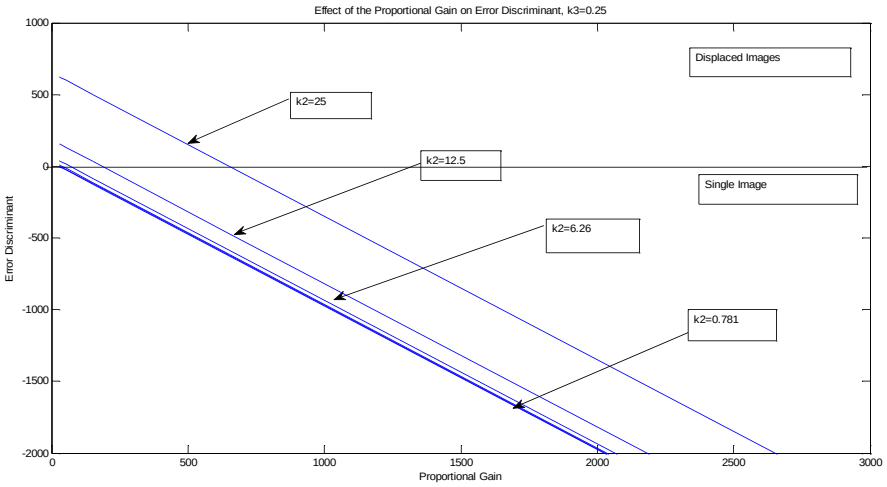

Figure 3: Error-gain Linkage

The effect of the discriminant, D, on the proportional controller gain, k_1, is summarized in Figure 3 for a fixed $k_{3\ and}$ parametric values of k_2. There is a bifurcation point between dual and single image behavior at D=0. With increasing k_2, the critical k_1 transition point shifts to higher values. This condition also delineates error structures as well. In prior papers the asymptotic hyperbolic responses of both the mean error and error standard deviation functions, as summarize in Figure 4, are discussed.

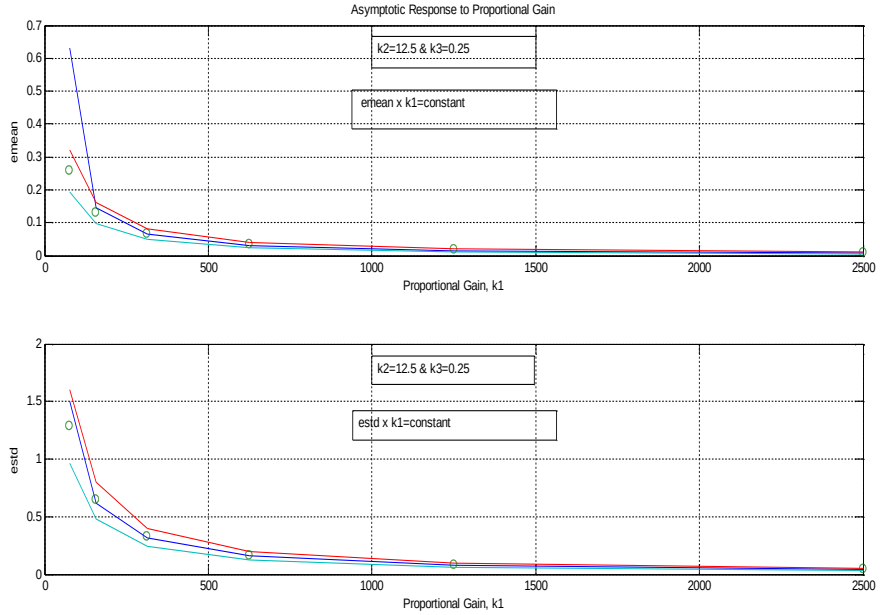

Figure 4: Asymptotic Behavior

Two models were developed for predicting the error pattern in the single image region. The first model devised was an Autoregressive Integrated Moving Average (ARIMA) where the seasonal structure was removed via a simple sinusoidal expression employing the critical locking frequency. The full/complete model was the sum of the empirical expression contribution and the ARIMA description of the non-seasonal noise structure. The second model retains the simple empirical expression but adds normal random noise with a mean and standard deviation matching the errors arising from a fit of the seasonal empirical model. These models are summarized in Table 1. The non-seasonal ARIMA model (2-0-2) parameters described in detail in Table 2 consist of two autoregressive and two moving average terms both of order one and two. No seasonal differencing was required. The Minitab (version 16) software package was used to estimate the model parameters.

Table 1: Non-Seasonal ARIMA Model

Final Estimates of Parameters

Type		Coef	SE Coef	T	P
AR	1	1.8771	0.0209	89.87	0.000
AR	2	-0.8782	0.0209	-41.99	0.000
MA	1	0.8661	0.0316	27.43	0.000
MA	2	-0.4395	0.0292	-15.03	0.000

Number of observations: 1000
Residuals: SS = 0.000255622 (backforecasts excluded)
MS = 0.000000257 DF = 996

Modified Box-Pierce (Ljung-Box) Chi-Square statistic

Lag	12	24	36	48
Chi-Square	46.9	59.5	84.2	87.7
DF	8	20	32	44
P-Value	0.000	0.000	0.000	0.000

Table 2: Non-Seasonal ARIMA Model Structures

		Seasonal		***Non-Seasonal***
$E_1\,(t)$	$=$	$A(k_1)\sin\left(\frac{\pi t}{200}\right)$	$+$	$z(t)$
		Seasonal		***Random***
$E_2\,(t)$	$=$	$A(k_1)\sin\left(\frac{\pi t}{200}\right)$	$+$	$\varepsilon(t)$

The non-seasonal ARIMA model (2-0-2) parameters described in detail in Table 2 consist of two autoregressive and two moving average terms both of order one and two. No seasonal differencing was required. The Minitab (version 16) software package was used to estimate the model parameters. A histogram of the ARIMA residuals are shown in Figure 5a and the normality is highlighted in Figure 5b. The large residuals observed in the tails of the normal probability plot are associated with early errors arising during the initial controller convergence phase. In addition the associated autocorrelation (ACF) and partial autocorrelation (PACF) plots (Figures 6a & 6b, respectively) indicate a reasonable data fit. Future studies will focus on improving the ARIMA modeling. Simulation results employing the respective devised models are shown in Figure 7 and in each case they are a good representation of the actual controller synchronization data.

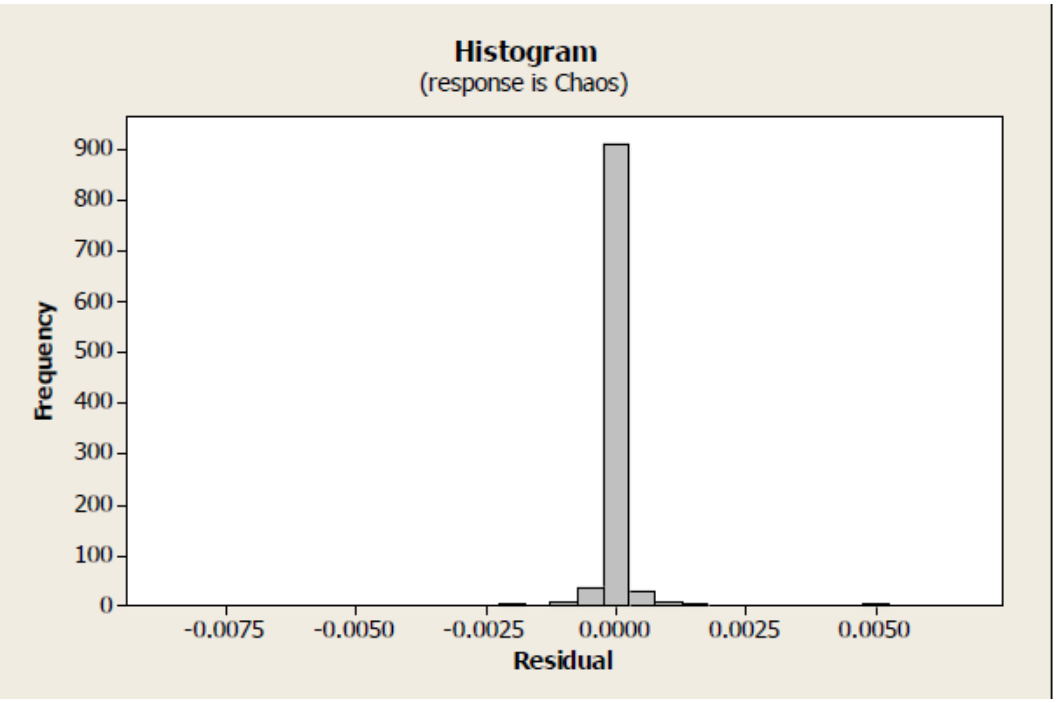

Figure 5a: ARIMA Residuals Plot

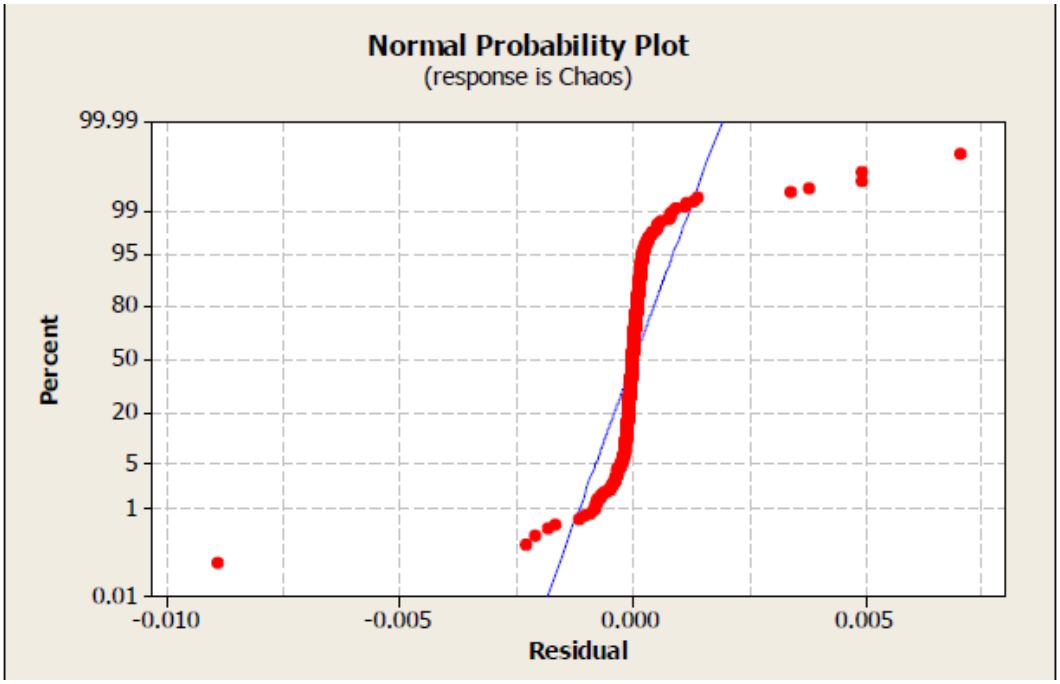

Figure 5b: ARIMA Residuals Normal Probability Plot

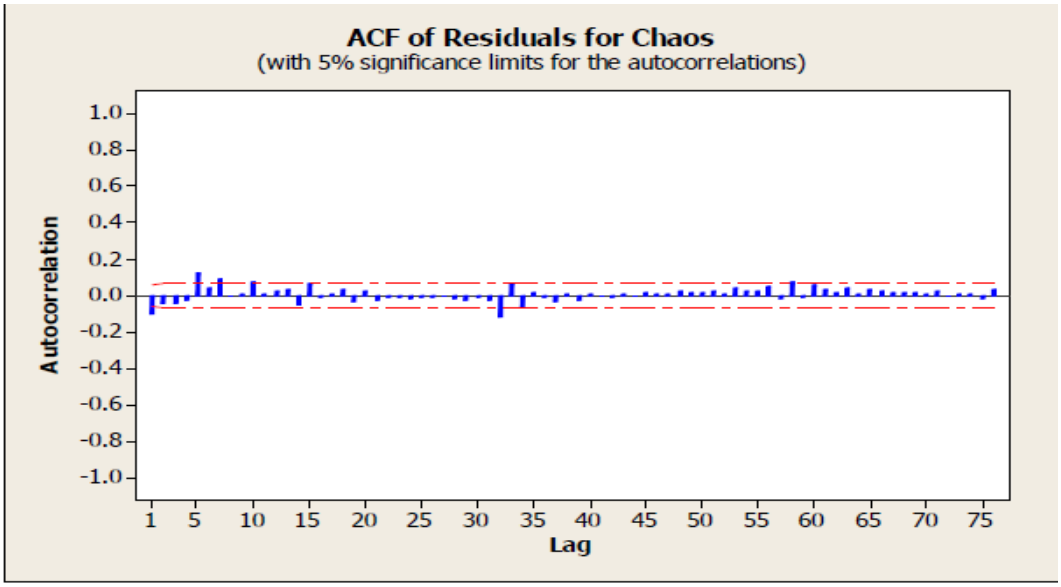

Figure 6a: ARIMA Residuals Autocorrelation Plot

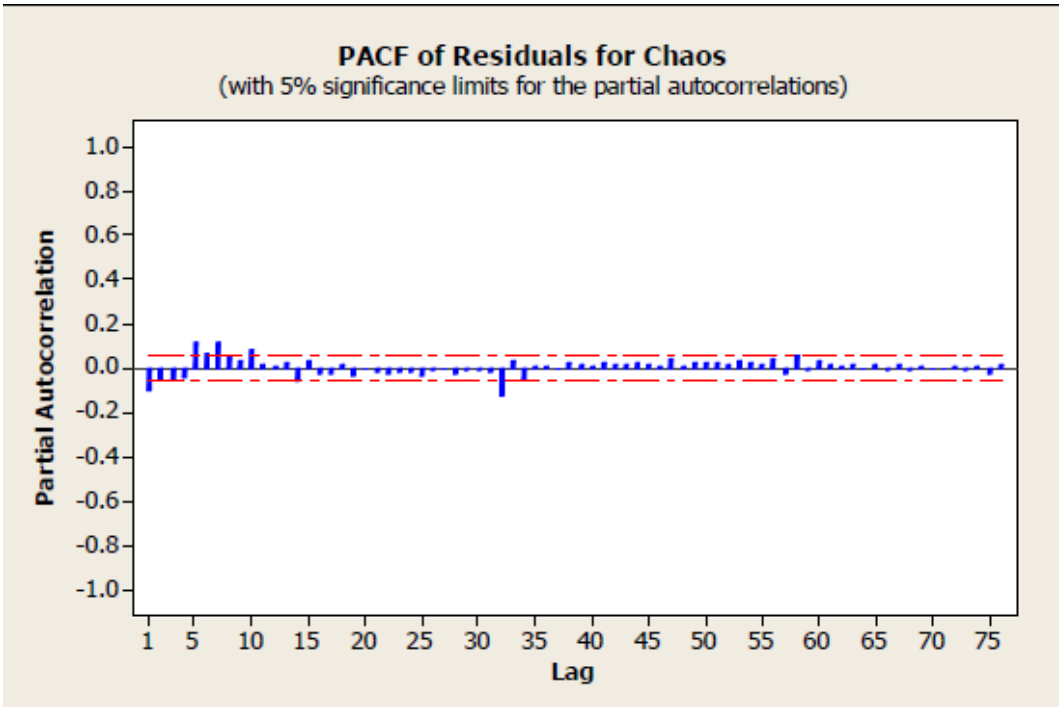

Figure 6b: ARIMA Residuals Partial Autocorrelation Plot

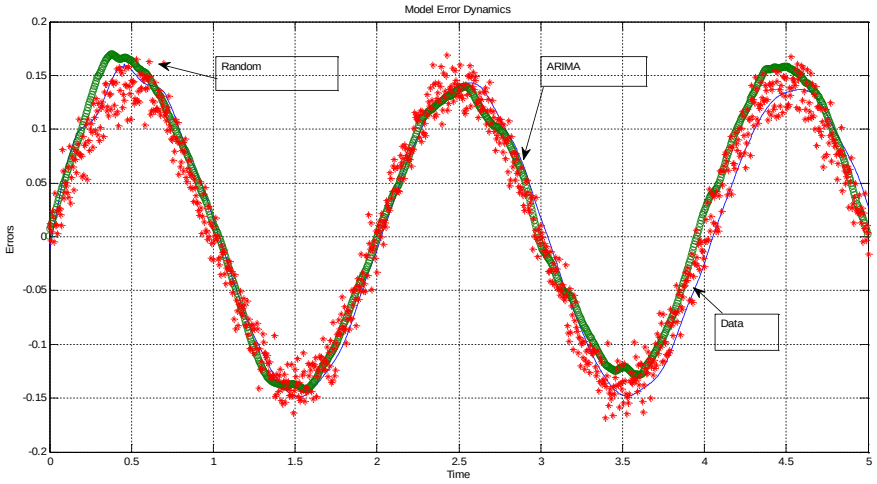

Figure 7: Predictive ARIMA Model Simulations

Conclusions

The error characteristic equation has a dominant effect on error structure. This unique equation also dictates controller requirements for the controller gains. It shows that two uniquely solutions are possible depending upon the sign of the discriminant associated with this equation. For discriminant values less than zero, an asymptotic error profile evolves with a fixed frequency. However, if the discriminant value is greater than zero, no discernible pattern is detected. Under conditions of fixed controller parameters for k_3 and $k_{2,}$ the error-gain linkage relationship is a linear one. An ARIMA 2-0-2 provides a reasonable description of the asymptotic error structure.

References

Bhiwani, R.J., & Patre B.M. (2011) *Design of Robust PI/PID Controller for Fuzzy Parametric Uncertain Systems.* International Journal of Fuzzy Systems, Vol. 13, No. 1, 16-23.

Boldrighini, C., & Franceschini, V. (1979). A Five-Dimensional Truncation of the Plane *Incompressible Navier-Stokes Equation.* Communications in Mathematical Physics, 64, 159-170.

Grzegorzewski, P. (2002). *"Nearest interval approximation of a fuzzy number,"* Fuzzy Sets and Systems, vol. 130, no. 3, 321-330.

Guan, S., Lai, C.H., & Wei, G.W. (2005). *Phase synchronization between two essentially different chaotic systems.* Physical Review E, 72, 016205.

Huang, D. (2005). *Simple adaptive-feedback controller for identical chaos synchronization.* Physical Review E, 71, 037203.

Huang, D. (2006). *Synchronization in Adaptive Weighted Networks*. Physical Review, 74, 046208.

Morgan III, M. H. & Morgan, C. B. (2011). *A Statistical Investigation of Swarm / Network Dynamics.* JSM Proceedings, Section on Physical and Engineering Sciences, Vancouver, British Columbia, July 30- August 3, 4567-4575.

Morgan III, M. H. & Morgan, C. B. (2012). *Using Novel Distance Metrics to Evaluate Statistical Robustness of Chaotic Control.* JSM Proceedings, Section on Physical and Engineering Sciences, San Diego, California, July 31- August 4, 2312-2320.

Morgan III, M. H. & Morgan, C.B. (2013). *Using Statistical Moments to Improve The Control of Chaotic Oscillators.* JSM Proceedings, Section on Physical and Engineering Sciences, Montreal, Canada, August 1-August 5, 3974-3983.

Morgan III, M. H. & Morgan, C.B. (2014). *Statistical Error-Based Controller Design of Hybrid System with Mixed Time Delays* JSM Proceedings, Section on Physical and Engineering Sciences, Boston, Mass, August 2-August 6, 3060-3068.

Mackey, D. & Glass, L.(1977), *Oscillations and Chaos in Physiological Control of Systems,* Science 197, 287-289.

Olgac, N. & Sipahi, R. (2002). Exact Method for the Stability of Time-Delayed Linear Time-Invariant (LTI) Systems, Transactions on Automatic Control, vol. 47, no. 5, 793-797.

Pecora, L.M., & Carroll, T.L. (1990*). Synchronization in Chaotic Systems*. Physical Review Letter, 64(8), 821-825.

Rekasius, Z. V. (1980). *A Stability Test for Systems with Delays,* Proc. Joint Automatic Control Conf., Paper No. TP9-A.

Sprott, J. C. (2003). *Chaos and Time Series Analysis*, Oxford University Press.